DOI: 10.13009/EUCASS2025-079
11TH EUROPEAN CONFERENCE FOR AERONAUTICS AND SPACE SCIENCES (EUCASS)

Species-Specific Vibrational Energy Model for Hypersonic Flow Simulations

Arun Kumar Chinnappan† *and Minkwan Kim*
Department of Aeronautics and Astronautics, University of Southampton, United Kingdom.
a.chinnappan@soton.ac.uk · m.k.kim@soton.ac.uk
†Corresponding author

Abstract

This work presents a species-specific vibrational energy model for hypersonic flow simulations. The translational-rotational modes are characterized by a single temperature, while the vibrational modes of individual diatomic molecules are treated separately. Vibrational-vibrational (V-V) energy exchange between unlike diatomic molecules is modelled using relaxation probabilities fitted to theoretical and experimental data from the literature. The model is validated using thermal bath test cases for both non-reacting and reacting flows, with comparisons against results from other continuum solvers, Direct Simulation Monte Carlo (DSMC), and high-fidelity state-to-state (STS) methods. Further validation is performed against experimental measurements for flow over a cylinder, demonstrating good agreement in terms of vibrational temperature profiles and shock stand-off distance.

1. Introduction

Hypersonic vehicles entering planetary atmospheres encounter a strong shock that results in a rapid rise in gas temperature. This increase in gas temperature excites the internal energy modes of the gas, leading to temperature differences between translational and internal modes - a condition known as thermal non-equilibrium. Moreover, high post-shock temperatures trigger complex chemical reactions, including dissociation, recombination, exchange and ionisation. When the timescales of internal energy relaxation and chemical reactions become comparable to the characteristic flow timescale, the flow is considered to be in a thermo-chemical non-equilibrium condition. This phenomenon significantly influences gas transport properties and reaction rates, ultimately affecting the overall flow field and heat flux predictions.[1,2] Therefore, high-fidelity modelling of hypersonic flows demands a detailed consideration of chemical kinetics and internal energy relaxation processes, necessitating the decoupling of different energy modes.

For non-ionising hypersonic flows (without electrons), the translational, rotational, vibrational, and electronic modes must be accounted for in the model. However, since translational-rotational modes and vibrational-electronic modes are often tightly coupled for di-atomic molecules, they can respectively be treated as single modes.[3] This led to the widely used Park's two-temperature model[3] in hypersonic computational fluid dynamics (CFD) that considers two temperatures to characterise all the modes: one for the translational-rotational modes and another for vibrational-electronic (V-E) modes. While this simplification is effective in many scenarios, using a single vibrational temperature for all diatomic species can be problematic. Different molecules relax at different rates;[4,5] for example, NO relaxes significantly faster than N_2. This discrepancy becomes especially critical during dissociation reactions, which are partially controlled by the vibrational temperature.

The limitations of the single-temperature assumption are further evident in high-enthalpy nozzle flows and rapidly expanding tubes.[6] As heated gas expands through a nozzle, it undergoes steep decrease in temperature and pressure. Because vibrational relaxation times differ significantly among species, their vibrational temperatures begin to diverge. For instance, N_2, with a slow relaxation rate, the vibrational temperature becomes frozen at the divergent section. As a result, the vibrational temperatures of different species vary significantly at the nozzle exit. These differences need to be accounted for while validating or testing the model for missions, particularly when modelling rapid flow expansions and comparing against data from ground-based experiments designed to simulate such conditions. Therefore, a detailed consideration of each vibrational mode is crucial for modelling hypersonic flows, either hypersonic flow over the body or rapid expansion flows.

In this work, we present a species-specific multi-vibrational model that accounts for the vibrational energies of individual molecules rather than a single temperature for all. Therefore, vibrational-translational (V-T) is accounted for by all the molecules, along with vibrational-vibrational (V-V) relaxation between unlike molecules. The V-V

DOI: 10.13009/EUCASS2025-079

relaxation rates are determined by fitting probabilities obtained from the literature. Due to their strong coupling, the translational and rotational modes are modelled with a single temperature. Electronic modes are included for diatomic molecules due to their contribution to vibrational energy. For atomic species, electronic modes are assumed to be in equilibrium with the translational temperature and are thus treated with a single temperature. Ionisation reactions and the associated free electron modes are not considered at this stage. These models are implemented in an in-house finite volume CFD solver developed at the University of Southampton, known as HANSA.[7] The validation process involves an initial comparison with hy2foam for a non-reacting flow, followed by comparisons against Direct Simulation Monte Carlo (DSMC) and high-fidelity state-to-state (STS) methods for a reacting flow. Finally, the model's predictions are compared with experimental data for temperature profiles and shock stand-off distance.

The reminder of this paper is arranged as follows: methodology is presented in Sec. 2, followed by results and discussions in Sec. 3 and conclusions are provided in Sec. 4.

2. Computational model

The conserved governing equations can be written in the following form:

$$\frac{\partial \mathbf{Q}}{\partial t} + \nabla \cdot (\mathbf{F} - \mathbf{F}_v) = \mathbf{S}_{NEQ} \tag{1}$$

where $\mathbf{Q}$ is the vector of conserved variables, $\mathbf{F}$ is the inviscid flux vector, and $\mathbf{F}_v$ is the viscous flux vector, $\mathbf{S}_{NEQ}$ is the thermo-chemical non-equilibrium source terms, $\mathbf{Q}$, is given by

$$\mathbf{Q} = \begin{pmatrix} \rho_1 \\ \rho_2 \\ \vdots \\ \rho_{ns} \\ \rho u \\ \rho v \\ \rho w \\ E \\ E_{v,1} \\ E_{v,2} \\ \vdots \\ E_{v,ns} \end{pmatrix} \tag{2}$$

where ρ_i is the density of species i, ns is the total number of species, u, v and w are flow velocities, E is the total energy, and E_v is the vibrational-electronic energy of individual molecular species. The electronic energies of atoms (N & O) are assumed to be in equilibrium with the translational temperature. The inviscid flux vector, $\mathbf{F}$, and viscous flux vector, $\mathbf{F}_v$, are expressed as:

$$\mathbf{F} = \begin{pmatrix} \rho_1 u \\ \rho_2 u \\ \vdots \\ \rho_{ns} u \\ \rho u \mathbf{U} + \delta_{ij} p \\ \rho v \mathbf{U} + \delta_{ij} p \\ \rho w \mathbf{U} + \delta_{ij} p \\ (E + p)\mathbf{U} \\ E_{v,1}\mathbf{U} \\ E_{v,2}\mathbf{U} \\ \vdots \\ E_{v,ns}\mathbf{U} \end{pmatrix} \tag{3}$$

DOI: 10.13009/EUCASS2025-079

$$\mathbf{F}_{v,i} = \begin{pmatrix} -J_{i,1} \\ -J_{i,2} \\ \vdots \\ -J_{i,s} \\ \tau_{i,x} \\ \tau_{i,y} \\ \tau_{i,y} \\ \tau_{ij}\mathbf{U}_j - (q_{tr} + \sum_s^{Allspecies} q_{v,s}) \\ -\sum(j_{i,s}h_s) \\ -q_{v,1} \\ -q_{v,2} \\ \vdots \\ -q_{v,ns} \end{pmatrix} \tag{4}$$

where δ_{ij} denotes the Kronecker delta, p is pressure, $J_{i,s}$ is species diffusion flux in the i^{th} direction, and τ_{ij} are components of the viscous stress tensor. q_{tr}, and q_{ve} are translational-rotational and vibrational heat flux, respectively. The viscous stresses are modelled using Stokes' hypothesis, assuming a Newtonian fluid, while heat fluxes for each energy mode are formulated based on Fourier's law. Species mass diffusion fluxes are modelled using the modified Fick's law, ensuring their sum is zero. Wilke's semi-empirical mixing rule is applied to determine mixture transport properties, including viscosity, diffusion coefficients, and thermal conductivity for each energy mode.

The thermochemical non-equilibrium source term, $\mathbf{S}_{NEQ}$, is described by

$$S_{NEQ} = \begin{pmatrix} \dot{\omega}_1 \\ \dot{\omega}_2 \\ \vdots \\ \dot{\omega}_s \\ 0 \\ 0 \\ 0 \\ 0 \\ S_{v,1} \\ S_{v,2} \\ \vdots \\ S_{v,ns} \end{pmatrix} \tag{5}$$

where $\dot{\omega}_s$ is the mass production rates of species s due to chemical reactions, and S_v is the vibrational energy source term for individual species.

The system of equations is solved within a finite volume (FV) framework. The Modified Steger-Warming (MSW) vector flux splitting approach is employed to construct inviscid fluxes, except at the shock, where the original Steger-Warming method is utilized. Viscous fluxes are calculated using a central scheme, with properties evaluated at the cell centres. Time integration is performed using a point-implicit algorithm.

2.1 Chemical Reactions

A finite-rate chemistry model involving five neutral species (N_2, O_2, N, O & NO) is considered in this work. The model includes dissociation, recombination and exchange reactions, and written as:
Dissociation and Recombination:

$$\begin{aligned} N_2 + M &\leftrightarrow 2N + M, \\ O_2 + M &\leftrightarrow 2O + M, \\ NO + M &\leftrightarrow N + O + M, \end{aligned}$$

where M can be N_2, O_2, N, O and NO.
Exchange reactions:

$$\begin{aligned} N_2 + O &\leftrightarrow NO + N, \\ NO + O &\leftrightarrow O_2 + N. \end{aligned}$$

DOI: 10.13009/EUCASS2025-079

The reaction rate constants for the reactions are taken from Ref. 3. The ionisation reactions are not considered in this work.

2.2 Multi-vibrational modelling

The vibrational energy source term, S_v, can be written as:

$$S_v = S_{chem} + S_{v-t} + S_{v-v} \tag{6}$$

where S_{chem} is the energy gained or removed due to chemical reactions, S_{v-t} is the energy transferred between translational and vibrational modes, and S_{v-v} is the vibrational energy exchange between unlike molecules. The vibrational energy added or removed by reactions is modelled using a non-preferential model as:

$$S_{chem} = \sum \dot{\omega}_s (e_{v,s} + e_{el,s}) \tag{7}$$

where $e_{el,s}$ is species electronic energy and $e_{v,s}$ is the average vibrational energy. The last two terms S_{v-t} and S_{v-v} in Eq. 6 are explained below.

2.2.1 Translational-Vibrational Relaxation

The vibrational-translational (V-T) energy exchange is modelled using the Landau-Teller formula[3] as:

$$S_{v-t} = \sum_s \rho_s \left(e'_{vs} - e_{vs}\right) / \tau_{vt}, \tag{8}$$

where e'_{vs} is the vibrational energy corresponds to the translational temperature. The relaxation time τ_{vt} can be expressed as $\tau_{vt} = \tau_{M-W} + \tau_{pc}$, where τ_{M-W} is Millikan-White correlation function[8] and τ_{pc} denotes Park's correction. In this work, the vibrational relaxation rates are determined using the modified Millikan-White parameters[9] along with Park's corrections.[3]

2.2.2 Vibrational-Vibrational Relaxation

The vibration-vibration energy transfer between species i and j is described as[10]

$$S_{v-v,i} = \sum_{j \neq i} P_{i,j} Z_{i,j} m_i \left(e_{v,i}(T'_{v,i}) - e_{v,i}(T_{v,i})\right), \tag{9}$$

where $P_{i,j}$ is the collision probability for V-V energy transfer, T'_v is the vibrational temperature of the two collision partners after the collision for V-V energy transfer, and Z is the collision number. The probability $P_{i,j}$ is set to 0.01 in Ref. 10, as this value was approached for N_2-NO and N_2-CO systems at temperatures greater than 3000 K in the experimental study by Taylor *et al.*[11]

In this work, we have curve-fitted the experimental and Schwartz-Slawsky-Herzfeld (SSH)[12] theory results by extracting data from Taylor *et al.*[11] The fits are given below:

$$P_{N_2-O_2} = 1.622 \times 10^{-14}\, T^{2.96} + 4.015 \times 10^{-10} \tag{10}$$

$$P_{N_2-NO} = 1.6936 \times 10^{-8}\, T^{1.38} \tag{11}$$

$$P_{O_2-NO} = 1.6936 \times 10^{-8}\, T^{1.38} \tag{12}$$

A similar type of fit was proposed in Ref. 13. These fits are shown in Fig. 1 along with the data from Taylor *et al.*[11] The probability of P_{O_2-NO} is assumed to be the same as that of P_{N_2-NO}, due to the lack of data for the former.

To demonstrate the importance of varying probability, the relaxation time over temperature at 1 atmospheric pressure for the present model is compared with the constant probability model and fit obtained through experiment from Streicher *et al.*,[5] as shown in Fig. 2. It is evident that using a constant probability significantly under-predicts the relaxation time at temperatures below 10 000 K; this indicates that the constant probability model results in excessively fast V-V relaxation. In contrast, the present model shows good agreement with the fit derived by Streicher *et al.*[5]

DOI: 10.13009/EUCASS2025-079

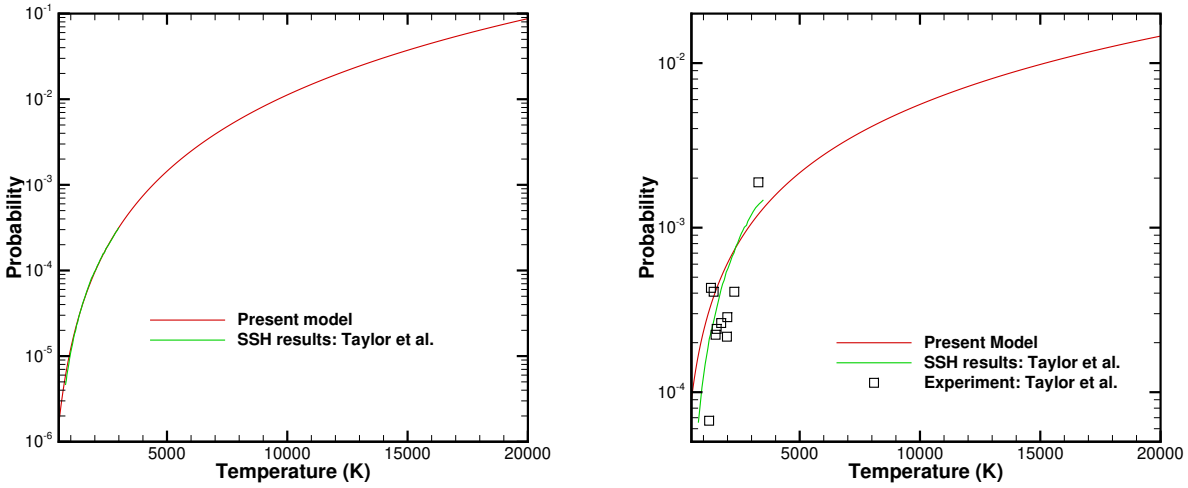

(a) N_2-O_2 (b) N_2-NO

Figure 1: V-V relaxation probabilities for N_2-O_2 and N_2-NO.

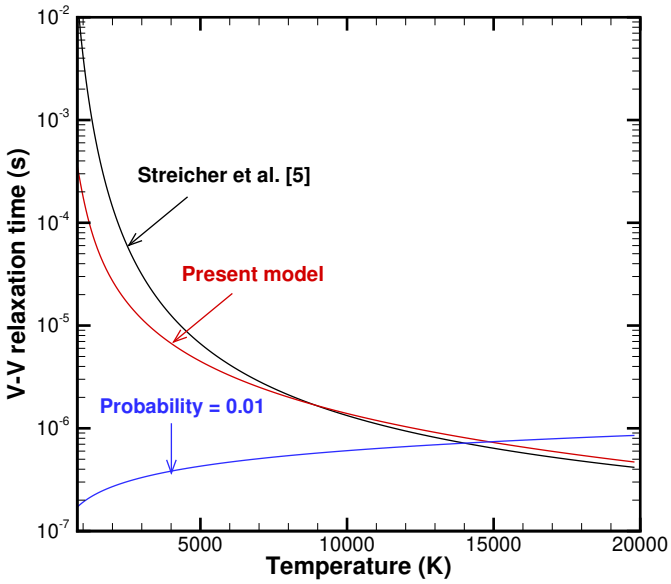

Figure 2: Variation of V-V relaxation time over temperature for N_2 - O_2 system at 1 atm pressure.

3. Results and Discussion

The proposed model is first validated for a non-reacting adiabatic thermal bath case. It is then compared with STS and DSMC results for a reacting case. Finally, the results are validated against the experimental data for flow over a cylinder.

3.1 Non-Reacting Flow

In this case, we validated the proposed model against hy2Foam by comparing the results with Casseau *et al.*[14] The test case involves a non-reacting thermal bath composed of N_2 and O_2, with flow conditions taken from Casseau *et al.*[14]

DOI: 10.13009/EUCASS2025-079

The initial translational-rotational and vibrational temperatures are set to 30 000 K and 5000 K, respectively, with a gas density of 0.0364 kg/m^3 for both N_2 and O_2. For consistency with Ref. 14, the V-V relaxation is switched off, and the Millikan-White model with Park's correction is employed. In all other cases, we consider V-V relaxation and use the modified Millikan-White model from Scalabrin *et al.*[1] The relaxation of translational and vibrational temperatures for N_2 and O_2 shows close agreement with hy2Foam. As seen in Fig. 3, O_2 relaxes faster than N_2, highlighting species-specific differences in relaxation rates. Eventually, all temperatures equilibrate at 12 128 K.

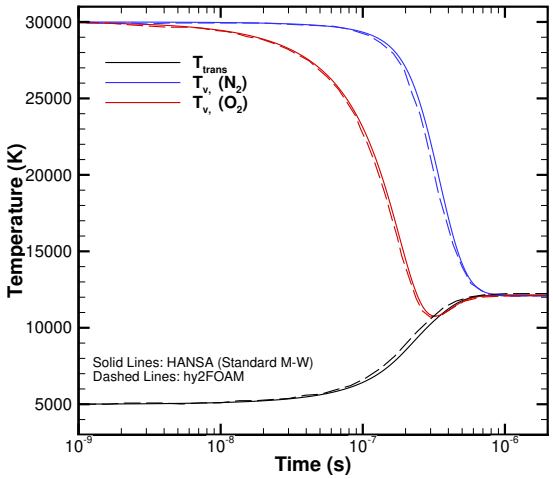

Figure 3: V-T relaxation of N_2 - O_2 system.

3.2 Reacting Flow

In this study, we compare the results from the proposed model with those obtained using STS and DSMC methods reported in the literature. The selected test case is a reacting thermal bath, referred to as Test Case 1 in Gimelshein *et al.*[15] The initial translational and vibrational temperatures are set at 7230 K and 300 K, respectively. The total density is 0.00204 kg/m^3, with an initial composition of N_2 and O_2 as 0.79 and 0.21, respectively. These conditions were taken in Ref. 15 as a replication of conditions behind a reflected shock in one of the experiments presented in Ref. 5. All the reactions mentioned in Sec. 2.1 are considered in this study. The gas undergoes adiabatic relaxation through energy exchange between different modes and chemical reactions, and the results are compared between different models.

The temporal evolution of the vibrational temperatures of N_2 and O_2 is compared against DSMC and STS results presented in Gimelshein *et al.*,[15] as illustrated in Fig. 4. The DSMC simulations were performed using the SMILE solver (referred to as DSMC-M2 in Ref. 15), which incorporates the discrete Larsen-Borgnakke model for V-T relaxation, quantum-classical trajectory (QCT) based approach for calculating vibrational collision numbers, and total collision energy (TCE) model for exchange reaction models. Dissociation and recombination reactions were modelled using the Bias method. Moreover, V-V relaxation was excluded in the DSMC simulations. The results show that the proposed model closely follows the trends observed in both STS and DSMC simulations. Given the absence of experimental data, the high-fidelity STS result is used as a reference. The present model demonstrates improved accuracy in predicting O_2 vibrational temperature compared to DSMC, whereas the agreement for N_2 is slightly less precise. The vibrational temperature profiles of O_2 and N_2 are comparatively closer for both the present model and STS than the DSMC results, where they are significantly more separated. This difference likely stems from the absence of V-V relaxation in the considered DSMC simulation. This closer agreement in the present model can be attributed to the inclusion of V-V relaxation, which promotes the redistribution of vibrational energy between the molecules. Figure 5 compares the vibrational temperature of O_2 obtained from the present model with STS, DSMC and experimental result. It is evident that the proposed model predictions are well within the experimental error values at all data points except the first value, where even the STS prediction exceeds the experimental measurement.

The temporal variation of translational and overall vibrational temperature of both single and multi-vibrational models is shown in Fig. 6. The overall vibrational temperature in the multi-vibrational model is computed as a mole-fraction weighted average of species-specific vibrational temperatures. While translational temperature profiles show negligible differences between the two models, a noticeable improvement is observed in the vibrational temperature

DOI: 10.13009/EUCASS2025-079

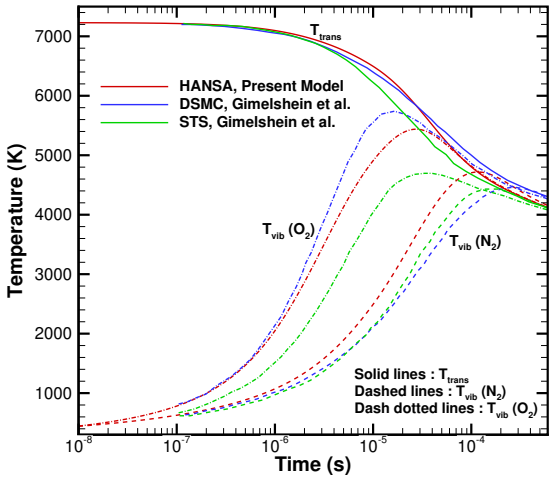

Figure 4: V-T relaxation for a reacting flow

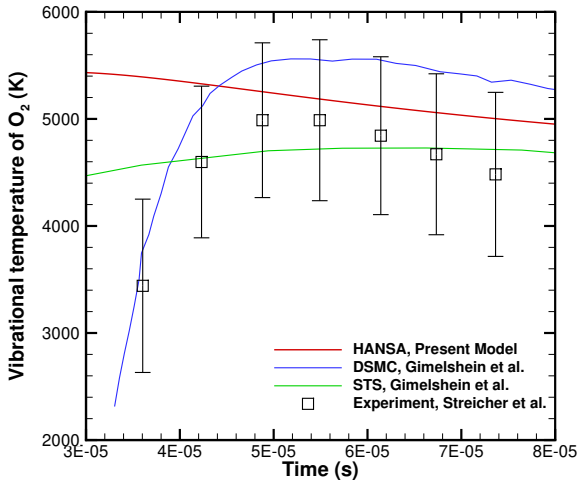

Figure 5: Comparison of O_2 vibrational temperature with DSMC, STS and experiment[5, 15]

predicted by the multi-vibrational model, bringing it closer to the STS predictions. The vibrational temperature in the single vibrational model is observed to relax quickly towards the translational temperature. Additionally, the time evolution of the mole fractions of NO and O is compared across all models, as shown in Fig. 7. It is evident that the proposed approach yields improved results compared to those from DSMC. While the difference between the single and multi-vibrational models is minimal, the later shows a slightly faster initial production of O. It is note that the STS results are plotted here are to show the improvement in the results due to multi-vibrational model, rather than a direct validation, as STS is a high fidelity expensive model and a perfect validation was not expected.

3.3 Flow over a flat faced cylinder

In this study, we simulated a flow through a nozzle, followed by its impingement on a flat faced cylinder, whose diameter is 50 mm and a length of 55 mm. This case is a replication of an experiment performed at DLR.[16] The nozzle inlet, throat and exit diameters are 75 mm, 29 mm, and 200 mm, respectively. The model is located at a distance of 200 mm from the nozzle exit. The inlet flow conditions are provided in Table 1 and the schematic figure is provided in Fig. 8. Thermal equilibrium is assumed at the inlet meaning that the vibrational temperatures of all the molecules are

DOI: 10.13009/EUCASS2025-079

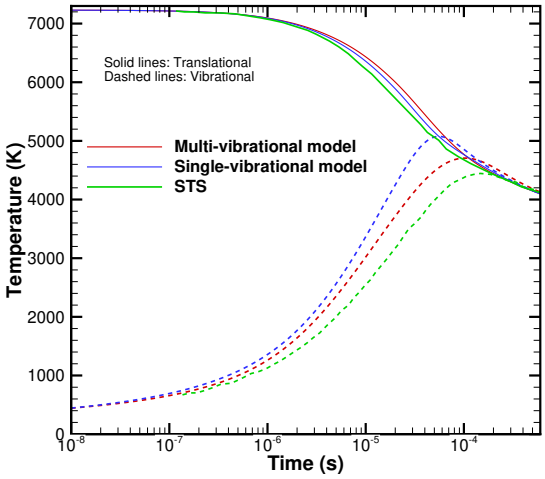

Figure 6: Comparison of temporal variation of single and multi-vibrational models along with STS results.

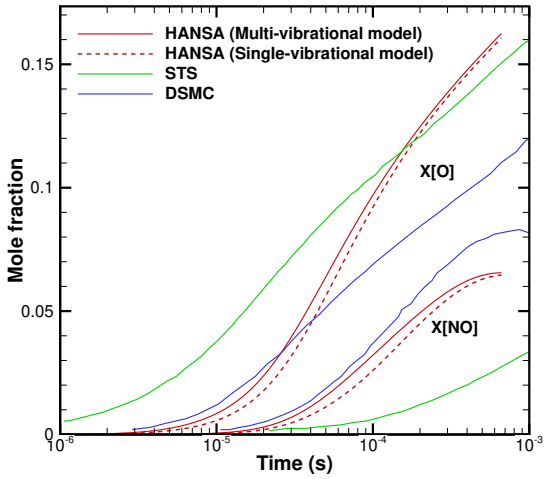

Figure 7: Temporal evolution of molar fractions of NO and O.

assumed to be the same as that of translational temperature.

Table 1: Flow conditions

Parameters	Values
Pressure, hPa	4350
Total temperature, K	5100
Mass fraction of N_2	0.737
Mass fraction of O_2	0.009
Mass fraction of NO	0.042
Mass fraction of N	0.009
Mass fraction of O	0.203

The spatial variation of translational (which is assumed to be the same as rotational in our model) and vibrational temperatures for individual species is shown in Fig. 9. As the flow expands through the nozzle, the temperature decreases for all modes. However, when the flow reaches the divergent section, the vibrational temperature of N_2 gets

DOI: 10.13009/EUCASS2025-079

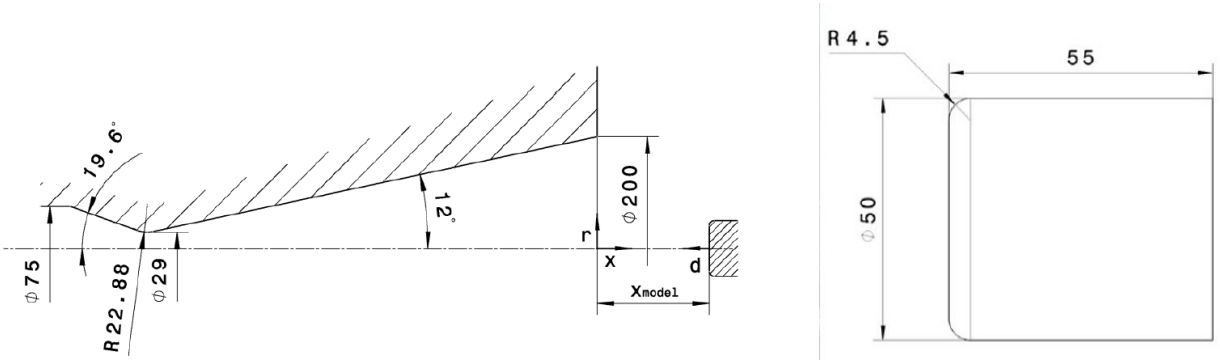

(a) Nozzle geometry along with the model

(b) Model geometry

Figure 8: Schematic view of the simulation (all units are in mm) taken from Gülhan *et al.*[16]

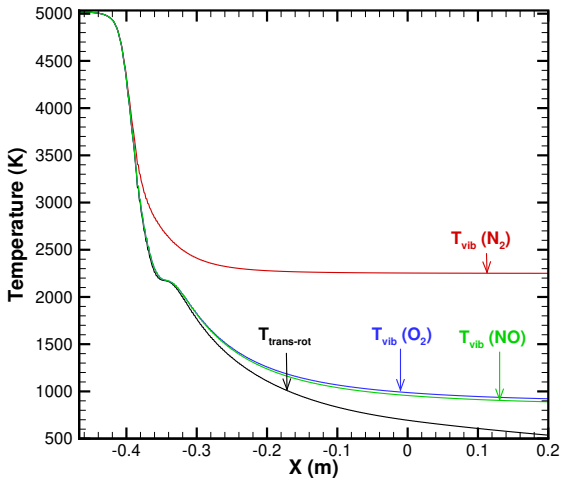

Figure 9: Temperature profile along the nozzle centerline for different energy modes.

frozen at approximately 2250 K. In contrast, the vibrational temperatures of O_2 and NO continue to evolve through the divergent section, relaxing towards the translational temperature. At the nozzle exit, the vibrational temperatures of N_2, O_2 and NO are observed to be 2250 K, 923 K, and 891 K, respectively. This significant difference in the vibrational temperatures of different molecules (that dictates the freestream conditions for the test model) could affect the flow behaviour such as shock structure and location, and heat transfer to the model. Therefore, to fully replicate experimental conditions and to quantify uncertainties in ground-based testing, species-specific vibrational modelling is crucial.

Figure 10 compares the translational and vibrational temperatures of different molecules predicted by the present model with the DLR's TAU CFD solver results.[16] Experimental measurements of the rotational temperature and the vibrational temperature of N_2, obtained through Coherent Anti-stokes Raman Spectroscopy (CARS) diagnostics, are also included in Fig. 10. The present solver accurately reproduces the vibrational temperature profile of N_2, showing excellent agreement with the experimental data. Furthermore, the predicted shock stand-off distance matches closely with the experimental observations. On the other hand, the TAU results slightly over-predict the peak temperature and underestimate the shock stand-off distance relative to the measured values.

4. Conclusion

We have presented a newly developed species-specific vibrational energy model that individually accounts for V-T relaxation and V-V relaxation among unlike molecules. The V-V relaxation probabilities were derived by fitting avail-

DOI: 10.13009/EUCASS2025-079

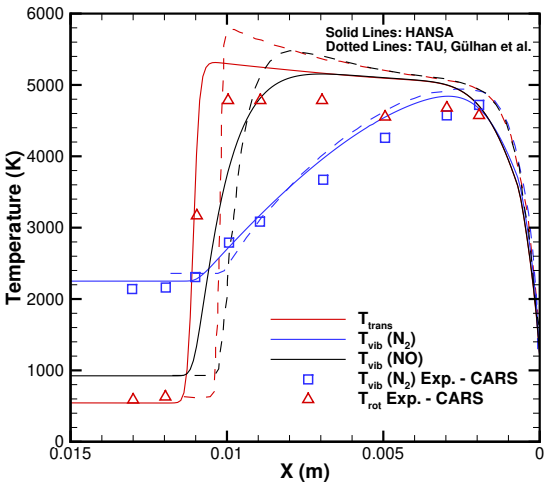

Figure 10: Comparison of temperature variation along the stagnation streamline with experiment and TAU results from Gülhan *et al.*[16]

able theoretical and experimental data from the literature. The model was implemented into the HANSA CFD solver and validated for non-reacting flow conditions. Detailed comparisons were performed against DSMC simulations and high-fidelity STS method for reacting flow. Finally, the model predictions were validated against experimental results, demonstrating good agreement in terms of shock stand-off distance and temperature profiles. Future work will focus on detailed analysing of the influence of the model in chemically reactions, including ionisation and electron non-equilibrium.

References

[1] Leonardo C Scalabrin. *Numerical simulation of weakly ionized hypersonic flow over reentry capsules*. PhD thesis, The University of Michigan, 2007.

[2] Nirajan Adhikari. *Investigation of Aerothermodynamic and Chemical Kinetic Models for High-Speed Nonequilibrium Flows*. PhD thesis, Purdue University, 2021.

[3] Chul Park. *Nonequilibrium Hypersonic Aerothermodynamics*. John Wiley & Sons, 1990.

[4] Jesse W Streicher, Ajay Krish, Ronald K Hanson, Kyle M Hanquist, Ross S Chaudhry, and Iain D Boyd. Shock-tube measurements of coupled vibration–dissociation time-histories and rate parameters in oxygen and argon mixtures from 5000 K to 10 000 K. *Physics of Fluids*, 32(7), 2020.

[5] Jesse W Streicher, Ajay Krish, and Ronald K Hanson. Vibrational relaxation time measurements in shock-heated oxygen and air from 2000 K to 9000 K using ultraviolet laser absorption. *Physics of Fluids*, 32(8), 2020.

[6] Ekaterina Nagnibeda and Elena Kustova. *Non-equilibrium reacting gas flows: kinetic theory of transport and relaxation processes*. Springer Science & Business Media, 2009.

[7] Thomas J Greenslade, Arun Kumar Chinnappan, and Minkwan Kim. Multi-physics simulation study of magnetic shielding on hypersonic vehicles. *CEAS Space Journal*, pages 1–12, 2024.

[8] Roger C Millikan and Donald R White. Systematics of vibrational relaxation. *The Journal of chemical physics*, 39(12):3209–3213, 1963.

[9] Chul Park. Review of chemical-kinetic problems of future nasa missions. I-earth entries. *Journal of Thermophysics and Heat transfer*, 7(3):385–398, 1993.

[10] Graham V Candler and Robert W MacCormack. Computation of weakly ionized hypersonic flows in thermochemical nonequilibrium. *Journal of Thermophysics and heat transfer*, 5(3):266–273, 1991.

DOI: 10.13009/EUCASS2025-079

[11] RL Taylor, M Camac, and RM Feinberg. Measurements of vibration-vibration coupling in gas mixtures. In *Symposium (International) on Combustion*, volume 11, pages 49–65. Elsevier, 1967.

[12] RN Schwartz, ZI Slawsky, and KF Herzfeld. Calculation of vibrational relaxation times in gases. *The Journal of Chemical Physics*, 20(10):1591–1599, 1952.

[13] Chul Park and Seung-Ho Lee. Validation of multitemperature nozzle flow code. *Journal of thermophysics and heat transfer*, 9(1):9–16, 1995.

[14] Vincent Casseau, Rodrigo C Palharini, Thomas J Scanlon, and Richard E Brown. A two-temperature open-source cfd model for hypersonic reacting flows, part one: zero-dimensional analysis. *Aerospace*, 3(4):34, 2016.

[15] Sergey F Gimelshein, Ingrid J Wysong, Alexander J Fangman, Daniil A Andrienko, Olga V Kunova, Elena V Kustova, Fabio Morgado, Catarina Garbacz, Marco Fossati, and Kyle M Hanquist. Kinetic and continuum modeling of high-temperature air relaxation. *Journal of Thermophysics and Heat Transfer*, 36(4):870–893, 2022.

[16] Ali Gülhan, Burkard Esser, Uwe Koch, Michael Fischer, Eggert Magens, and Volker Hannemann. Characterization of high-enthalpy-flow environment for ablation material tests using advanced diagnostics. *AIAA Journal*, 56(3):1072–1084, 2018.